

Nanoscale Mechanosensing of Natural Killer Cells is Revealed by Antigen-Functionalized Nanowires

Guillaume Le Saux, Netanel Bar-Hanin, Avishay Edri, Uzi Hadad, Angel Porgador, and Mark Schwartzman*

Cells sense their environment by transducing mechanical stimuli into biochemical signals. Commonly used tools to study cell mechanosensing provide limited spatial and force resolution. Here, a novel nanowire-based platform for monitoring cell forces is reported. Nanowires are functionalized with ligands for cell immunoreceptors, and they are used to explore the mechanosensitivity of natural killer (NK) cells. In particular, it is found that NK cells apply centripetal forces to nanowires, and that the nanowires stimulate cell contraction. Based on the nanowire deformation, it is calculated that cells apply forces of down to 10 pN, which is the smallest value demonstrated so far by microstructured platforms for cell spreading. Furthermore, the roles of: i) nanowire topography and ii) activating ligands in the cell immune function are studied and it is found that only their combination produces enhanced population of activated NK cells. Thus, a mechanosensing mechanism of NK cells is proposed, by which they integrate biochemical and mechanical stimuli into a decision-making machinery analogous to the AND logic gate, whose output is the immune activation. This work reveals unprecedented mechanical aspects of NK cell immune function and introduces an innovative nanomaterial for studying cellular mechanics with unparalleled spatial and mechanical resolution.

Cells sense mechanical properties of their environment by converting physical forces into biochemical signals.^[1,2] During the last two decades, extensive research efforts have aimed at exploring cellular force sensing mechanism, mostly in the context of adhesion receptors.^[3–7] In addition, it became progressively clear that mechanical forces also regulate the immune


function of cells.^[8] These forces have different origins, such as actin dynamics,^[9] and play important roles at different stages of the lymphocyte immune activity. Initial sampling of antigens on the surface of antigen presenting cells (APCs), as well as activation of immunoreceptors, strongly depends on actin polymerization and dynamics.^[10] Moreover, immunoreceptors recognize antigens under mechanical load to discriminate between high-affinity and low-affinity antigens.^[11] Once activated, the receptor–antigen complexes on the lymphocyte–APC interface are driven by retrograde actin flow and myosin contraction into highly regulated structures termed immune synapse, whose forces affect the inside-out signaling of lymphocytes. Today, mechanical forces in immune system are a subject of emerging research, which has so far mostly focused on T cells and B cells.^[12,13]

Studying mechanical forces in cells is challenging, because these forces have relatively low magnitude – mostly at the nanoNewton scale, and often span over miniature regions sized down to the molecular scale. Existing tools include optical traps,^[14,15] micropipettes,^[16] and atomic force microscopy (AFM),^[17,18] which, however, apply and detect forces only at single point on the cell membrane, and do not overview the mechanical behavior of the entire cell. Alternatively, traction force microscopy, which determines the displacement of microbeads embedded in hydrogel surface for cell spreading, maps forces of entire cells,^[19–21] however, it can hardly detect the exact bead movement since the beads are distributed randomly, and their resting position is unknown. Furthermore, analysis of bead movement requires complex force calculations based on elasticity theory.^[22] These constraints can be overcome by elastomeric micropillars for cell spreading, which allow facile mapping of force distribution within cells.^[23] Furthermore, micropillars can be functionalized with biomolecules that yield chemical stimuli for various cell functions, such as adhesion^[24,25] or immune response,^[26] and thereby allow integration of mechanical and biochemical cues. However, the advantages of elastic micropillars come at the expense of their spatial and mechanical resolution. Indeed, poly(dimethyl siloxane) (PDMS) – material of choice for micropillar fabrication – is limited for the fabrication of pillars with micrometer-scale size and aspect ratio of 3:1, for which sensing forces below

Dr. G. Le Saux, N. Bar-Hanin, Dr. M. Schwartzman
Department of Materials Engineering
Ben-Gurion University of the Negev
Beer Sheva 84105, Israel
E-mail: marksc@bgu.ac.il

Dr. G. Le Saux, N. Bar-Hanin, Dr. U. Hadad, Dr. M. Schwartzman
Ilse Katz Institute for Nanoscale Science & Technology
Ben-Gurion University of the Negev
Beer Sheva 84105, Israel

A. Edri, Prof. A. Porgador
The Shraga Segal Department of Microbiology
Immunology and Genetics
Faculty of Health Sciences
Ben-Gurion University of the Negev
Beer Sheva 84105, Israel

 The ORCID identification number(s) for the author(s) of this article can be found under <https://doi.org/10.1002/adma.201805954>.

DOI: 10.1002/adma.201805954

the nanoNewton scale is arduous. Interestingly, Ghassemi et al. have recently demonstrated that the cellular response produced by micrometer-scale pillars was fundamentally different from that of $1/2\ \mu\text{m}$ pillars, since the latter could spatially resolve forces of localized myosin fibers.^[27] Thus, the cellular forces monitored by miniaturized pillars do not necessarily scale with the pillar size in a linear fashion. These findings emphasize the critical need in a tool that could monitor forces within cells with the nanometric resolution, and help reveal details invisible by existing tools such as micropillars.

Nanowires are quasi-1D nanomaterials with sub-100 nm diameter, and during the last two decades they have been extensively explored as building blocks for nanodevices, mostly for the applications in electronics,^[28,29] photonics,^[30] energy harvesting,^[31] and chemical- and biosensing.^[32] Recently, nanowires have been also demonstrated for the ultrahigh resolution mechanical sensing in cells.^[33,34] However, integration of chemical cues with nanowires has not been shown yet, and the insight regarding nanowire–cell interaction remains limited. Here, we report a novel nanowire-based platform for the detection and monitoring of cell forces, which integrates both mechanical and chemical cues. The nanometric radius and ultrahigh aspect ratio of nanowires allowed us to monitor cell forces with ultrafine mechanical and spatial resolutions. We used this platform to explore mechanosensitivity of natural killer (NK) cells – lymphocytes of the innate immune system – whose mechanoregulation has been mostly unexplored up to date. Notably, nanowire topography mimics to certain extent the surface of antigen, presenting cells such as dendritic cells with whom NK cells come in contact, as discussed in more details at the end of this letter. To enable antigen-specific interaction between the nanowires and NK cells, we functionalized the nanowires with major histocompatibility complex I (MICA) – ligands that are recognized by NKG2D activating receptors of NK cells (Figure 1a). We stimulated NK cells on MICA-functionalized nanowires, and found that nanowires permit enhanced cell contraction, whereas such contraction is impossible on flat surfaces functionalized with MICA. We used high resolution fluorescence microscopy and scanning electron microscopy (SEM) to discover that NK cells anchor and bend nearby nanowires during their stimulation (Figure 1b). Based on the magnitude of the nanowire bending, we assessed that the mechanical load applied by NK cells on a single nanowire is of the order of 10 pN, which is one order of magnitude smaller than the minimal force which can be detected by elastomeric micropillars.^[26]

Finally, we studied the effect of: i) nanowire topography and ii) MICA immobilization on the immune function NK cells. We found that while each of these two factors alone was insufficient to stimulate significant cell immune response, their combination substantially boosted NK cell degranulation. This finding indicates that NK cells use mechanical forces to sense their environment, and that this sensing is based on an independent mechanotransduction pathway which is costimulatory to the chemical signaling. In this sense, NK cells can be analogous to a Boolean AND gate, whose independent mechanical and chemical signaling provides two logic inputs. Our findings provide an important insight into the underlying mechanism of NK cell immune function, as well as demonstrate a novel toolbox for detecting cellular forces with an unprecedented spatial and mechanical resolution.

Vertical ZnO nanowires (Figure 2a) were grown on A-plane sapphire in a home-made chemical vapor deposition system (see the Supporting Information and refs. [35,36]). We calibrated the nanowire growth conditions to yield nanowires with an average diameter of 50 nm (Figure S1, Supporting Information) and length of 20 μm . We grew nanowires from catalyst nanoparticles obtained by thermal dewetting of thin Au film, calibrated to produce continuous nanowire array of an average surface density of ≈ 9 nanowires μm^{-2} , as obtained from SEM images (Figure 2a). This density ensures that despite the nonuniform nanowire distribution at a short range, each cell is exposed to numerous nanowires that induce a cumulative mechanical stimulus. To explore the effect of the nanowire topography on NK cell function, we compared NK cells stimulated on nanowires to NK cells stimulated on control “flat” surfaces, which were made of Si wafers covered with 50 nm Au nanoparticles, with an average surface density of a few tens of nanoparticles per 100 μm^2 , as characterized by AFM (Figure S2 and the Supporting Information). Both nanowire and flat surfaces were functionalized with the MICA ligand. In addition, we used the following control samples: i) bare (nonfunctionalized) surfaces of both types, and ii) surfaces functionalized with a negative-control ligand (small Ubiquitin-like modifier; SUMO), henceforth referred to as “mock ligand.” In total, these six types of cell activation platforms (Figure 2b) were designed to separately and independently elucidate the effect of nanowires and ligands on the immune activation of NK cells.

To functionalize nanowires with ligands, we took advantage of the ability of ZnO to chemisorb.^[37–39] We functionalized ZnO nanowires with a commercially available thiol terminated by

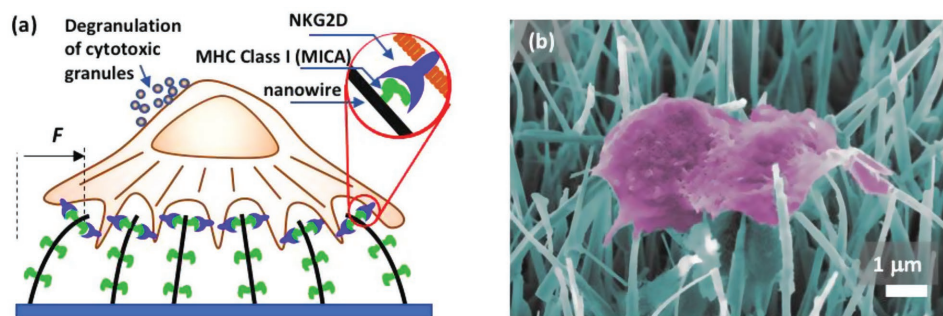


Figure 1. a) Schematic drawing of NK activation on MICA-functionalized nanowires. b) SEM of NK cells on MICA-functionalized nanowires.

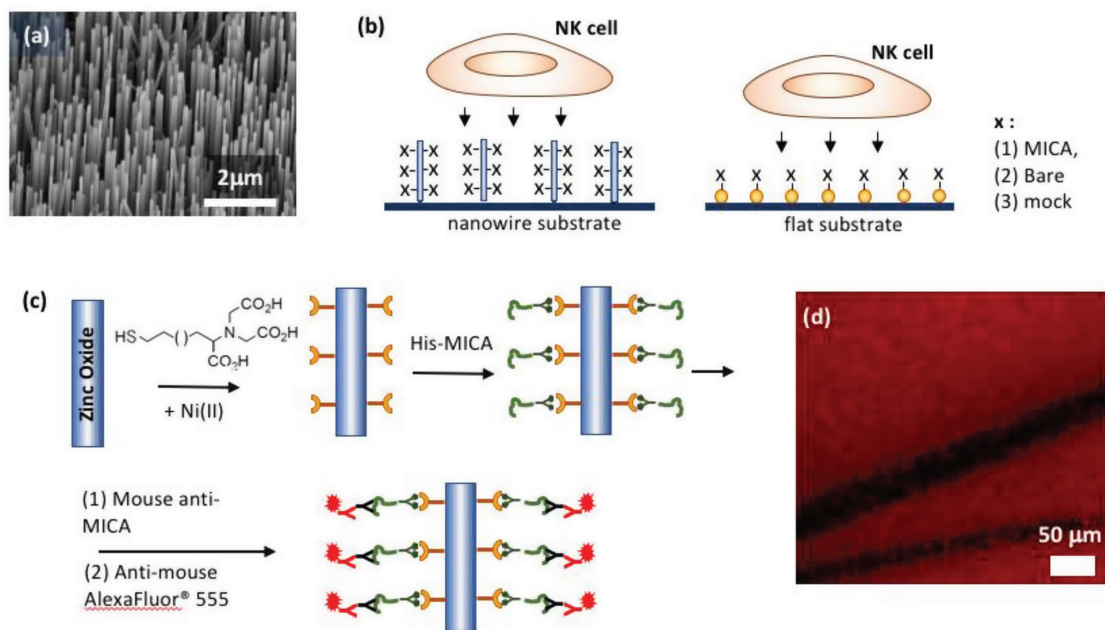


Figure 2. a) SEM of vertical ZnO nanowires. b) Schematic drawing of 6 types of samples used for the activation of NK cells. c) Nanowire functionalization with MICA. d) Immunostaining of MICA-functionalized nanowires: fluorescence image of a surface covered with MICA-functionalized and fluorescently immunostained nanowires. Two scratches in the nanowire array expose the bare sapphire surface with no immobilized MICA.

nitrilotriacetic acid (NTA), followed by its chelation with Ni, and further attachment of His-conjugated ligand (Figure 2c, see the Supporting Information for details). We used the same protocol to functionalize Au nanoparticles on flat surfaces. We confirmed the site specificity of our functionalization by indirect MICA immunofluorescence, using Alexa 568-conjugated anti-mouse as the secondary antibody. To better detect the fluorescence signal from the functionalized nanowires, we intentionally produced a few scratches within the nanowire forest. We found that the scratched areas, which were lacking nanowires, did not produce any fluorescence signal, confirming that MICA is immobilized on nanowires but not on sapphire surface (Figure 2d). Interestingly, while focusing on sapphire surface, we could observe distinct parallel fluorescent lines, which were a few tens of micrometers long (Figure S4, Supporting Information). We concluded that these lines are horizontal ZnO nanowires that epitaxially grew along the $\pm[1\bar{1}00]$ sapphire direction.^[35,40] The high fluorescence contrast of these nanowires with sapphire background confirms that the functionalization is selective to ZnO, and uniform along the nanowire. In addition, two less complex experimental group unrelated to NK cell functions were used to prove the selectivity of thiol-based functionalization of ZnO nanowires: i) immobilization of labeled avidin via biotin terminated monolayer (Figure S5, Supporting Information), and ii) decoration of the nanowires with Au nanoparticles via thiol-terminated monolayer (Figure S6, Supporting Information).

To find whether the nanotopography produced by nanowires affects the function of NK cells, we first assessed the impact of nanowires on the cell spreading. To that end, we incubated NK cells on MICA-functionalized nanowires and on the control surfaces for 3 h, fixed the cells, stained their cytoskeleton with phalloidin to clearly visualize the cell contour, and

measured their projected area using fluorescence microscopy (Figure 3). During the sample preparation and the cell experiments, we took great care keeping samples in liquid to avoid drying effect, which could bend nanowires. We should note that cells on nonfunctionalized and mock-functionalized flat had similar projected areas to that of cells suspended in medium (Figure S7, Supporting Information). Even though the area on mock-functionalized nanowires is slightly higher than on the mock-flat surface, this difference is not statistically significant ($p = 0.2055$, see the Table S1 in the Supporting Information for the full statistical analysis). Thus, these surfaces did not stimulate cell spreading. Alternatively, MICA-functionalized nanoparticles stimulated cell spreading $\approx 2\text{--}3$ times higher when compared to the other flat surfaces (Figure 3a). The observed enhancement of cell spreading on MICA-functionalized flat surface can be interpreted through the activation mechanism of NKG2D. NKG2D signals by making a complex with transmembrane protein DAP10.^[41,42] Within the DAP10 cytoplasmic domain, a Src homology 2 (SH2) domain binding recruits the p85 subunit of the phosphatidylinositol 3-kinase (PI3K).^[43,44] Activated PI3K binds to the small adaptor CrKL, which activates GTPases Rac1 and Rap1 through binding to guanine nucleotide exchange factor, and thereby promotes spreading.^[45,46] Notably, recent studies have shown that spatial distribution of surface-immobilized activating ligands regulates spreading of T cells.^[47,48] Furthermore, we have recently demonstrated that NK cell spreading requires a minimal spatial distribution of MICA ligands.^[49] Based on the results obtained here, we conclude that the control surfaces with MICA-functionalized nanoparticles contained enough MICA to trigger a pronounced spreading of NK cells.

The most intriguing result, however, is the average projected area of NK cells on MICA-functionalized nanowires, which was

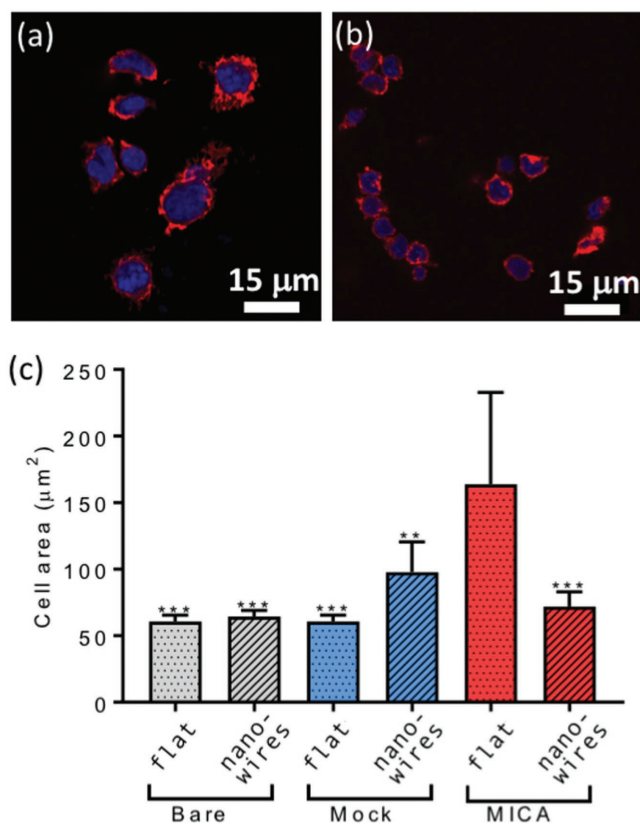


Figure 3. Cell spreading. a,b) Representative images of NK cells on MICA-functionalized flat surface and MICA-functionalized nanowires, respectively. Cell area was quantified by measuring the projected area of the cell cytoskeleton. c) Results are shown. Analysis of variance and Tukey's post hoc test were performed to assess the significant changes in behavior. We compared the projected area of flat-MICA surface to the other surfaces. The difference was considered statistically significant for $p < 0.05$. Two asterisks denote a p -value range of 0.001–0.01. Three asterisks equate to a p -value range of 0.0001–0.001. The minimal number of inputs was $N = 4$.

about 2.5 times smaller than that obtained on the MICA-functionalized flat surface (Figure 3b,c). Also, similar average areas were obtained for cells on bare and mock-functionalized nanowires. Based on these findings, we conclude that when NK cells are placed on nanowires, their spreading is mostly regulated by the nanowire topography, and not by the ligands immobilized onto the nanowires. In other words, the effect of surface topography overruled the effect of chemistry. We also believe that the nonuniform distribution of nanowires has a negligible effect on the variation cell spreading. Indeed, we recently studied NK cell spreading on ordered nanoarrays of ligands, and observed similar variation in the cell area, which is likely inherent to the cells.^[49] This finding can be interpreted in terms of global mechanical compliance of the underlying surface to the forces generated by cells. Indeed, it is well established that stiffer surfaces better simulate cell spreading due to their resistance to the tension within the membrane induced by cell contraction.^[50–53] We assume that the array of vertical high-aspect-ratio nanowires provides an extremely mechanically compliant environment, which provides minimal resistance to cell contraction.

To better understand how nanowire topography affects cell spreading, a deep insight into the interaction of NK cells with nanowires is needed. Notably, previous reports on interaction of various cells with inorganic nanowires showed that nanowires can predominantly penetrate the cell membrane,^[54–57] or invaginate the membrane,^[58,59] depending on the cell and nanowire types. Furthermore, adding functional chemistry—such as adhesion molecules—onto the nanowire surface can modulate the cell–nanowire interaction.^[60] Naturally, understanding how nanowires interact with NK cells is critical for analyzing and interpreting the results described here.

We fixed the cells after 3 h of incubation onto MICA-functionalized nanowires, dried in critical point drier, and imaged them in high-resolution SEM (Figures 1b and 4a). It can be clearly seen that the cells lay on top of the nanowires, being in contact with their upper $\approx 2 \mu\text{m}$. It is also seen that the nanowires do not penetrate the top cell membrane. Yet, SEM images cannot tell whether the nanowires penetrate the bottom cell membrane and access the cytosol or invaginate the membrane. To address this question, we stained the membrane and cytoskeleton of cells spread on MICA-functionalized nanowires with CellMask plasma membrane stain (green) and phalloidin (red), respectively, and imaged them by confocal microscopy. Z-stack images (top view, Figure 4b) clearly show green lines of $\approx 2 \mu\text{m}$ in length, which are projections of the membrane that surround the nanowires. These membrane projections, together with the lack of penetrating nanowires in SEM images, indicate that nanowires do not puncture the membrane but invaginate it.

The centripetal direction of membrane projections confirms that cells trap and bend neighboring nanowires, as was previously observed by SEM. The nanowire contours are also seen on XZ and YZ cross-sections of the confocal images. It should be noted that similar nanowire projections of the stained membrane were observed for NK cells on bare and mock-functionalized nanowires (Figure 4c,d). The way by which NK cells bend neighboring nanowires, which prior to exposure to the cells were perfectly vertical (as seen in Figure 2 a), clearly indicates that the cells apply centripetal forces onto the nanowires during their spreading. The high compliance of the nanowires to these forces thus induces a smaller spreading. Again, cells spread on bare, MICA-functionalized, and mock-functionalized nanowires were found to bend nanowires in a similar way, and to contract to nearly the same projected areas. Based on this finding, we conclude that NK cells apply mechanical forces onto their environment using a distinct mechanism which is independent of the incoming chemical signaling. Notably, some clustered nanowires outside the cells are observed in the SEM images in Figures 1b and 4a, despite the samples having been dried in a critical point drier. Careful inspection reveals the presence of what appear to be cell debris at the tips of the clustered nanowires, some of which was probably left by motile NK cells. Still, we believe that these debris have a negligible effect on the ability to detect cell forces using nanowires.

The detailed mechanism of how NK cells apply forces on their environment still needs to be understood. Previous force studies of epithelial and fibroblast cells using elastomeric micropillars showed that actin couples to adhesions on the pillar tops, and flows to produce centripetal forces.^[24,27] Later,

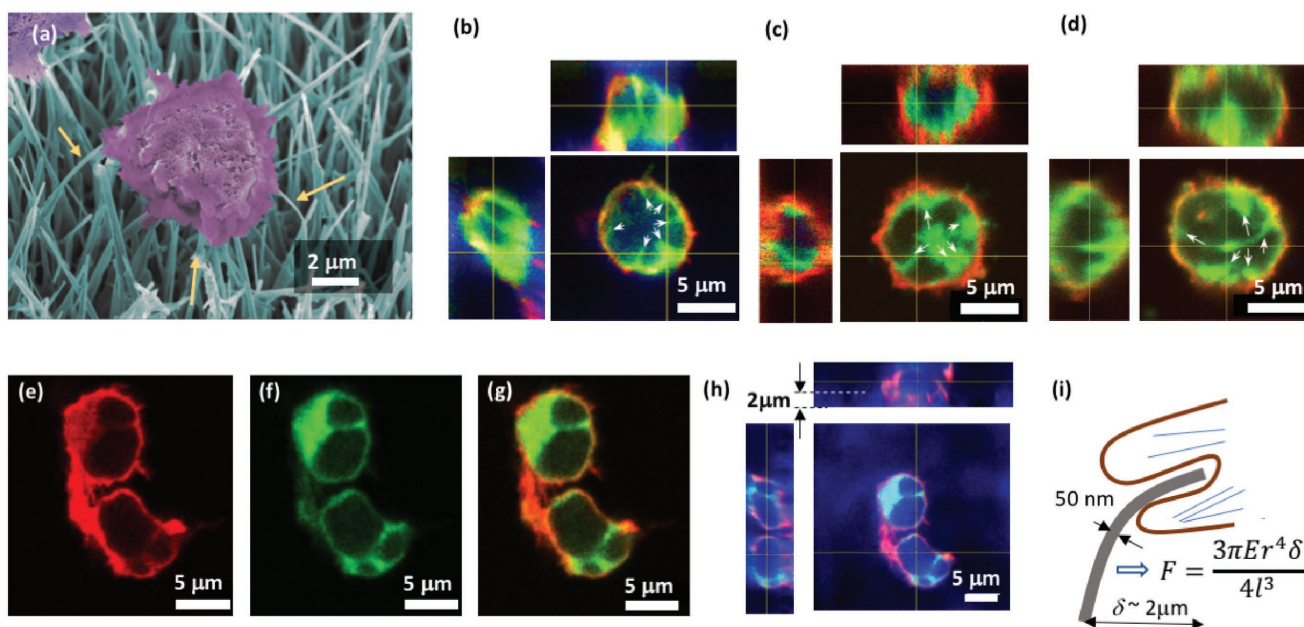


Figure 4. a) SEM image of a NK cell spread on MICA-functionalized nanowires. The yellow arrows point at the nanowires bent upon centripetal forces applied by the cell. b–d) Z stack of confocal microscopy of NK cells with tagged membrane onto MICA-functionalized, bare, and mock-functionalized nanowires, respectively. Cell membrane (green) and actin (red). The white arrows point onto the projected invaginations of the nanowires in the cell membrane. e) Cytoskeleton image of NK cells on MICA-functionalized nanowires. f) Membrane image of the same cells. g,h) Merging of (e) and (f), showing colocalization of the cytoskeleton and membrane when wires invaginate NK cells, and thereby indicating the concentration of acting along the invaginated nanowires. i) Calculation of the force applied by NK cell onto a single nanowire.

similar force studies of T cells using micropillars with immobilized activating antibodies showed that actin couples to the T-Cell Receptor–Cluster of Differentiation 3 (TCR–CD3) complexes on the pillar tops, suggesting that T cell force generation is associated with these complexes, and shares features with integrin-mediated force generation.^[26] Here, we found that actin was concentrated on the cell periphery, as well as on the nanowire projections, colocalizing with the membrane protrusions (Figure 4e–g and Figure S8 (Supporting Information)). This finding is mirrored by the abovementioned studies of fibroblast, epithelial, and T cell mechanosensing, and suggests that force generation in NK cells involves extensive actin polymerization in the vicinity of the nanowire invaginations. Interestingly, ZnO is a wide-gap semiconductor intrinsically fluorescent in blue and near-blue regions.^[61] Here, the emitting ZnO nanowires are visible on the Z-stack cross-sections with enhanced blue channel, confirming that the invaginations are $\approx 2 \mu\text{m}$ deep (Figure 4h), i.e., the top 10% of 20 μm long nanowires are in contact with cells.

The forces exerted by NK cell on individual nanowires can be quantified through the magnitude of the nanowire deflection, using a formula for bending a cantilever with circular cross-section^[62]

$$F = \frac{3\pi E r^4 \delta}{4l^3} \quad (1)$$

where F is the force, l is the nanowire length, E is the Young's modulus, δ is the nanowire horizontal deflection, and r is the nanowire radius. Notably, classical physics often fails to predict properties and behavior of nanoscale objects because of their

extremely high surface-to-volume ratio. Indeed, both experimental and theoretical studies showed size dependence of nanowire bending Young modulus due to surface roughness, surface stress, and the native oxidation layer; however, this size dependence is significant only for nanowires whose diameter is below 50 nm.^[63] In this research, we will use nanowires with the diameter of ≈ 50 nm or slightly above, for which classical theory of elasticity is applicable. For the calculation, we used a typical nanowire length of 20 μm , and a radius of 50 nm (Figure 4i). The reported bending Young modulus for ZnO nanowires ranged from ≈ 30 to ≈ 60 GPa, depending on the measurement.^[64–67] Here, we used the average modulus value of 45 GPa to estimate the force applied on a single nanowire. The average nanowire deflection roughly estimated from both fluorescence and SEM images (Figure 4a–h) was $\approx 2 \mu\text{m}$. In this case, the calculated force applied on an individual nanowire is about 10 pN. This value provides an important insight onto the nanoscale mechanics of NK cells. Yet, beyond this insight, it also demonstrates the great potential of nanowires as a platform for monitoring cell forces in general. Notably, elastomeric pillars previously used to quantify forces in spread cells^[16] can be downsized to 1/2 μm diameter,^[27] which is close to the miniaturization limit of PDMS fabrication. On the contrary, nanowires are few tens of nanometers in diameter, and thus allow to monitor cell forces with spatial resolution that is an order of magnitude higher than that achievable by PDMS pillars. Furthermore, nanowires have an extremely high aspect ratio – 400 in our case. Therefore, although made of a rigid material, individual vertical nanowire, as well as their ensemble, possesses an exceptionally high mechanical compliance, and responds to ultrasmall forces by relatively large bending. 10 pN is, to the

best of our knowledge, the smallest force that has been quantified using a micro-/nanostructured surface for cell spreading. For comparison, PDMS micropillars used to study mechanosensing of T cells could reveal forces in the order of 100 pN.^[26]

NK cells are the sentinels of the innate immune system, and contribute to immunity by cytolysis, cytokine secretion, and regulation of adaptive responses. NK cells recognize tumor, virus-infected, or stressed cells,^[68] and attack them by directed exocytosis of perforins and granzymes, and secretion of cytokines.^[69] The cytotoxicity of NK cells is regulated by the gentle balance of activating and inhibitory receptors that determines whether a target cell will be tolerated or attacked.^[70] However, our understanding of the activation mechanism of NK cells is limited to its biochemical signaling aspects. Very recently, Barda-Saad and co-workers indicated that mechanical signals regulate NK cell function by demonstrating that actomyosin retrogrades flow controls of NK cell immune response.^[71] Yet, the exact mechanism of how NK cells generate and sense mechanical forces is still unclear.

To understand whether NK cells sense the mechanical properties of nanowires, and whether this sensing regulates

the NK cell immune function, we monitored the expression of lysosome-associated membrane protein-1 (CD107a) in the cells activated on MICA-functionalized nanowires, as well as on the control surfaces. In activated NK cells, lytic granules are transported to the immune synapse, fused to the membrane, and degranulated at the membrane surface. During the degranulation, CD107a molecules are exposed to the outer side of the membrane, allowing to use CD107a as a quantitative marker for NK cell immune response.^[72,73] Staining of surface-expressed CD107a and its fluorescence imaging is a broadly used and proven method to detect the immune activation of NK cells, as well as other lymphocytes.^[74–76] Such a detection is impossible either by western blot which will expose cytosolic CD107a, or by flow cytometry that would require cell detachment from the nanowires which may change the cell shape, and thus lose all information on mechanosensing. Here, we imaged CD107a by staining NK cells with its fluorescently tagged monoclonal antibody, after 3 h of incubation (Figure 5a,b). Notably, the cells were not permeabilized to avoid diffusion of CD107a antibody into their cytosol and labeling of internal CD107a.

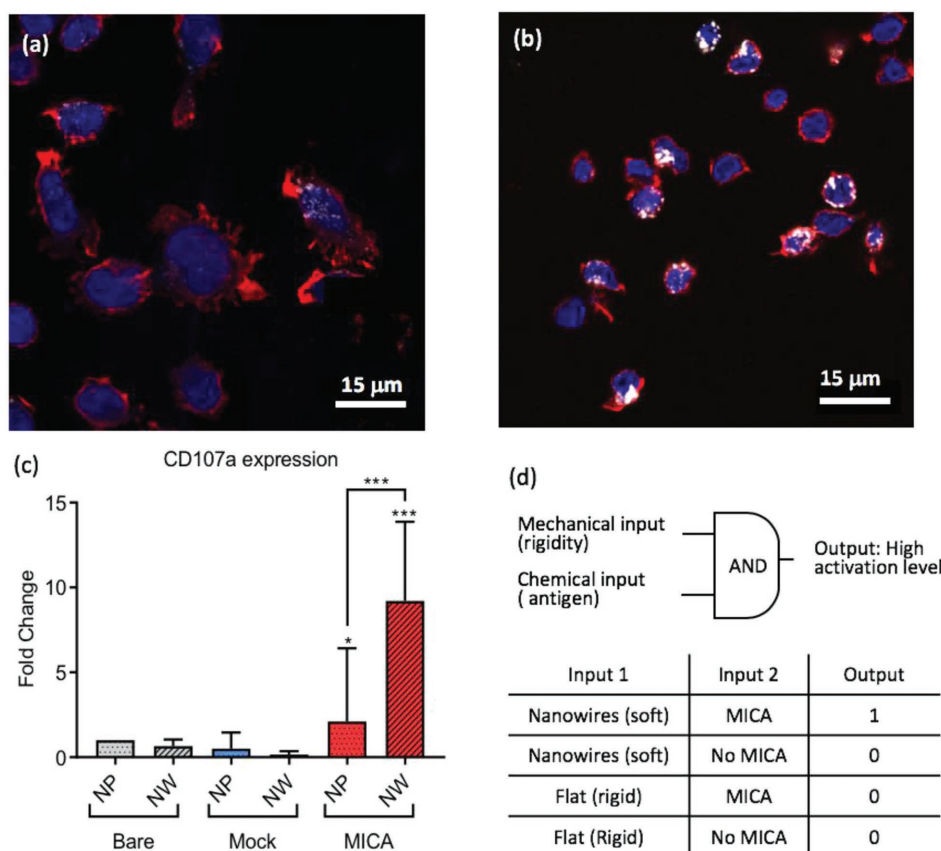


Figure 5. Cell activation. a,b) Representative images of NK cells on MICA-functionalized nanoparticles (NP-MICA) and MICA-functionalized nanowires (NW-MICA), respectively. c) Degree of CD107a expression was quantified by measuring the fluorescence intensity of the APC-labeled anti-CD107a (in white in (a) and (b)). Collected value for fluorescence intensity were normalized to the unmodified nanoparticle (NP-Bare). Analysis of variance and Tukey's post hoc test were performed to assess the significant changes in behavior. NP-Bare was chosen as reference for the post hoc test. An additional post hoc test was performed to compare the values between NP-MICA and NW-MICA. The results were considered significant for $p < 0.05$ (one asterisk in (c)). Three asterisks equate to a p -value range of 0.0001–0.001. The minimal number of inputs for each group was 4. d) Scheme and truth table of AND logic gate implemented by the activation of NK cell.

We found that MICA immobilization on both flat and nanowire-covered surfaces is essential for the degranulation of NK cells (Figure 5c). Furthermore, we found that MICA-functionalized nanowires stimulated a fourfold higher expression of CD107a compared to MICA-functionalized flat surfaces. To verify whether this difference stems from a possible discrepancy in the amount of MICA on flat and nanowire surfaces, we immunostained both the surfaces with fluorescent secondary MICA antibody, and compared the intensity of fluorescence signals. Surprisingly, we found that the flat surface produces a 3 times higher fluorescence signal than that of the surface covered with nanowires. Thus, the flat surface contained nearly 3 times more MICA than the one with nanowires. Furthermore, based on our previous finding that NK cells were contact only with approximately top 10% of the nanowires, and that MICA is immobilized uniformly along the nanowire surface (Figure S9, Supporting Information), we can conclude that cells on nanowires were exposed to ≈ 30 times less MICA than those on flat MICA surface. Still, the effect of the nanowire topography and flexibility on NK cell activation seems to overrule the effect of MICA quantify. On the other hand, the results obtained from nonfunctionalized and SUMO-functionalized nanowires clearly show that nanowires alone, i.e., without MICA, did not suffice to produce a significant immune response.

We suggest that the enhanced activation of NK cells on MICA-functionalized nanowires indicates that NK cells use mechanical forces to probe their environment. Our finding is mirrored by the recently demonstrated mechanosensing ability of other lymphocytes, such as T cells and B cells, which were studied on surfaces with different rigidities. Interestingly, the immune response of these cells to surface rigidity was found to be dependent on the cell and surface types. For example, T cells activated in antigen-functionalized hydrogels with a Young modulus below 200 kPa increased their immune response with an increase in surface rigidity,^[8] whereas T cells activated on antigen-functionalized PDMS with a Young modulus up to 2 MPa showed the opposite trend.^[77] Also, B cells were reported to increase their immune activation with an increase in surface rigidity ranging below 22 kPa.^[78] Similar to these studies, this work provides evidence that NK cells sense the mechanical features of their environment. The exact mechanism of this sensing is yet to be elucidated. It is possible that mechanical forces modify the downstream signaling of NKG2D, and perhaps of other receptors, and affect the formation of the immune synapse in NK cells. Notably, mechanotransduction at focal adhesions has been extensively studied during the last two decades. Many of the focal adhesion proteins, such as vinculin, paxillin, talin, and Pyk2, are also involved in the immune synapse of NK cells.^[79] These proteins may thus be involved in the mechanosensing mechanism of NK cells.

Our results clearly indicate that the mechanical signaling alone is not sufficient to stimulate an immune response, but must be combined with a biochemical signal, such as that provided by MICA ligands. Notably, lymphocytes express a repertoire of activating receptor whose engagement requires independent activation of costimulatory receptors. In recent years, combining orthogonal activating and costimulatory signaling pathways has been harnessed to engineer AND-gate T cells with precisely tuned therapeutic discrimination.^[79–81]

Here, we created a set of environmental conditions in which NK cells behave like an AND logic gate, whose two inputs – chemical and nanomechanical – define the immune outcome (Figure 5d). The logic 1 (true) output is defined as the increase of CD107a expression for at least one order of magnitude as compared to nonactivated NK cells.

As we mentioned before, nanowire shape, mechanical properties, and arrangement, can greatly impact cell behavior. For instance, it was recently shown that variations in the nanowire geometry and density alter the response of cultured epithelial and cancer cells.^[82] Similarly, different responses to different nanowires were described for neurons.^[34,83] Furthermore, Shalek et al. showed that the penetration of different cells by nanowires depends on the cell type and nanowire dimensions.^[54] In particular, they showed that silicon nanowires which were 2–3 μm long and up to 150 nm in diameter penetrated the membrane of primary NK cells. Interestingly, they demonstrated that those Si nanowires, which were substantially shorter and thicker than the nanowires used in the present paper, neither deflected upon the forces applied by NK cells, nor induced an immune response of NK cells. Conversely, in the present work, we deliberately produced nanowires with a relatively small diameter of 50 nm and high aspect ratio to ensure that they would not penetrate the cell membrane, and would be highly compliant to small forces exerted by cells. We analyzed the bending compliance, which is defined as the ratio of the lateral nanowire deflection to the applied bending force, and can be calculated using the formula given in Figure 4i, for the two types of compared nanowires. We found that for ZnO nanowires with a typical length of 20 μm and diameter of 50 nm used in the present work, the bending compliance is 193 kN m^{-1} , while for Si nanowires with the typical length of 2.5 μm and diameter of 150 nm used by Shalek et al., the compliance is 1.27 N m^{-1} . This more than fivefold difference in the mechanical compliance, which stems mostly from the different geometries of the compared nanowires rather than from the difference between the Young moduli of Si (1.65 GPa^[84]) and of ZnO, is among the key reasons for the different functional behavior of NK cells described in the two papers. This comparison clearly shows that geometry and physical properties of nanowires can largely regulate the response of NK cells. In particular, we believe that the minimal invasion of nanowires into the cell membrane, as described in this paper, ensured that survival rate of NK cells in our experiments was close to 100%, as was indicated by negligible amount of cell debris on the nanowires in SEM images.

Besides a possible role of the nanowire morphology and mechanical properties in the immune function of NK cell, high clustering of the MICA ligands on the nanowire surface might also stimulate NK cell activation. Indeed, the overall density of MICA on the flat control surface was substantially higher than on nanowires, yet the MICA molecules are immobilized on evenly dispersed nanoparticles. By contrast, MICA molecules immobilized on nanowires formed highly concentrated clusters. These clusters could lead to the high agglomeration of NKG2D at the cell–nanowire interface, which would in turn enhance NK cell activation. Interestingly, in vivo, activated NK cells interface APCs by forming the immune synapse. The periphery of the NK synapse contains phosphotyrosine-rich

NKG2D–DAP10 microclusters, that move toward the synapse center, where they lose the phosphotyrosine signal.^[85] However, a flat 2D synapse structure is unlikely possible on the surface of MICA-functionalized nanowire. Our activation results demonstrate that although NKG2D clusters differently on nanowires and within an in vivo synapse, both the clusters share similar functional features that stimulate degranulation of NK cells. We believe that the MICA-functionalized nanowires used here allow two processes which are vital for NK cell activation in vivo: clustering of ligand at the nanowires (as shown in Figure S4 in the Supporting Information) and mobility of these clusters stemming from the flexibility of the wires (as shown in the SEM and fluorescence images in Figure 4). In addition, nanowire invaginations change of the morphology of membrane and surrounding cytoskeleton. These changes alone can possibly produce a stimulus to enhance NK cell activation. To separately probe the effect of invagination and mechanical compliance to the forces, an experimental system in which these two parameters can be varied independently is required. Engineering such a system, which may consist, for instance, of nanowires with varied bending moduli but similar invagination depths, is the subject of our ongoing studies.

The receptor clustering on nanowires may have a certain in vivo relevance. Recent morphological studies of the immune synapse in T cells showed a structure consisting of nanosized elongated protrusions (podosomes), which are formed both on the T cell membrane and APC membrane.^[86] Furthermore, NK cells are activated by dendritic cells through the formation of a stimulatory synapse in the cell–cell interface.^[87] Dendritic cells are notable for the distinct branched projections on their surface, which resemble nanowires in their size, scale, and shape, and which transform during the cell maturation to villi by cytoskeletal rearrangement.^[88] The role of the surface nanotopography and nanomechanics of dendritic cell in the immune activation of NK cells, as well as other lymphocytes, is mostly unclear. Nanowires functionalized with antigens can mimic the nanotopography of dendritic cell surface. Systematic variations in the nanowire dimensions and shape, achievable by their growth conditions, can be harnessed for the study of how dendritic cell nanotopography regulates NK cell activation. Furthermore, such a study does not have to be limited to NK cells, and can be extended to other important components of the immune systems, such as T cells and B cells.

In summary, our study demonstrates that nanowires in combination with antigen functionalization can regulate the function of immune cells. This novelty paves the way to utilizing nanowires as a unique experimental platform to harness the nanoscale mechanisms of cell immune activity. Furthermore, due to their small diameter and high aspect ratio, nanowires allow force monitoring in cells with unique spatial and mechanical resolution. Finally, we provided the direct evidence for the nanoscale mechanosensing of NK cells, and its role in immune activity. Importantly, besides the impact of our findings on the fundamental understating of NK immune function, and, in particular, the mechanical features the NK immune synapse, they may also have practical importance. Shaping NK cell antitumor activity by ex vivo upregulation of their activating receptors is an emerging strategy for NK-cell-based adaptive immunotherapy. To that end, NK cells are cultivated in the

presence of cytokines, accessory cells, or feeder cells, which control the obtained NK cell phenotype.^[89] Enhanced NK cell activation on antigen-functionalized and mechanically stimulating nanotopography, as demonstrated here through nanowires, foreruns novel nanoengineered platforms for cell expansion toward therapeutic purposes, with improved efficiency and control of their cytotoxic activity.

Supporting Information

Supporting Information is available from the Wiley Online Library or from the author.

Acknowledgements

G.L.S. and N.B.H. contributed equally to this work. The authors thank Prof. Mira Barda-Saad from the Bar-Ilan University, Israel, for fruitful discussion. This work was funded by the Multidisciplinary Research Grant – The Faculty of Health Science in Ben-Gurion University of the Negev and Israel Ministry of Science and Technology: Israel-Taiwan Collaborative Grant # 3-12409, Israel Science Foundation, Individual Grant # 1401/15, and Israel Science Foundations: F.I.R.S.T. Individual Grant # 2058/18. The paper was written through contributions from all authors.

Conflict of Interest

The authors declare no conflict of interest.

Keywords

biofunctionalization, mechanosensing, nanowires, NK cells

Received: September 13, 2018

Revised: November 6, 2018

Published online: November 28, 2018

- [1] V. Vogel, M. Sheetz, *Nat. Rev. Mol. Cell Biol.* **2006**, *7*, 265.
- [2] V. Vogel, M. P. Sheetz, *Curr. Opin. Cell Biol.* **2009**, *21*, 38.
- [3] C. S. Chen, J. Tan, J. Tien, *Annu. Rev. Biomed. Eng.* **2004**, *6*, 275.
- [4] M. L. Gardel, I. C. Schneider, Y. Aratyn-Schaus, C. M. Waterman, *Annu. Rev. Cell Dev. Biol.* **2010**, *26*, 315.
- [5] M. P. Sheetz, *Nat. Rev. Mol. Cell Biol.* **2001**, *2*, 392.
- [6] R. Oria, T. Wiegand, J. Escribano, A. Elosegui-Artola, J. J. Uriarte, C. Moreno-Pulido, I. Platzman, P. Delcanale, L. Albertazzi, D. Navajas, X. Trepal, J. M. García-Aznar, E. A. Cavalcanti-Adam, P. Roca-Cusachs, *Nature* **2017**, *552*, 219.
- [7] P. Roca-Cusachs, A. del Rio, E. Puklin-Faucher, N. C. Gauthier, N. Biais, M. P. Sheetz, *Proc. Natl. Acad. Sci. USA* **2013**, *110*, E1361.
- [8] E. Judokusumo, E. Tabdanov, S. Kumari, M. L. Dustin, L. C. Kam, *Biophys. J.* **2012**, *102*, L5.
- [9] M. L. Dustin, *Curr. Opin. Cell Biol.* **2007**, *19*, 529.
- [10] M. Barda-Saad, A. Braiman, R. Titerence, S. C. Bunnell, V. A. Barr, L. E. Samelson, *Nat. Immunol.* **2005**, *6*, 80.
- [11] E. Natkanski, W.-Y. Lee, B. Mistry, A. Casal, J. E. Molloy, P. Tolar, *Science* **2013**, *340*, 1587.
- [12] R. Basu, M. Huse, *Trends Cell Biol.* **2017**, *27*, 241.
- [13] W. A. Comrie, J. K. Burkhardt, *Front. Immunol.* **2016**, *7*, 68.

- [14] H. Kress, E. H. K. Stelzer, D. Holzer, F. Buss, G. Griffiths, A. Rohrbach, *Proc. Natl. Acad. Sci. USA* **2007**, *104*, 11633.
- [15] M. Footer, J. Kerssemakers, J. Theriot, M. Dogterom, *Proc. Natl. Acad. Sci. USA* **2007**, *104*, 2181.
- [16] R. Basu, B. M. Whitlock, J. Husson, A. Le Floc'h, W. Jin, A. Olyer-Yaniv, F. Dotiwala, G. Giannone, C. Hivroz, N. Biais, J. Lieberman, L. C. Kam, M. Huse, *Cell* **2016**, *165*, 100.
- [17] M. Prass, K. Jacobson, A. Mogilner, M. Radmacher, *J. Cell Biol.* **2006**, *174*, 767.
- [18] F. Kong, A. J. García, A. P. Mould, M. J. Humphries, C. Zhu, *J. Cell Biol.* **2009**, *185*, 1275.
- [19] S. Munevar, Y. L. Wang, M. Dembo, *Biophys. J.* **2001**, *80*, 1744.
- [20] B. Sabass, M. L. Gardel, C. M. Waterman, U. S. Schwarz, *Biophys. J.* **2008**, *94*, 207.
- [21] W. R. Legant, C. K. Choi, J. S. Miller, L. Shao, L. Gao, E. Betzig, C. S. Chen, *Proc. Natl. Acad. Sci. USA* **2013**, *110*, 881.
- [22] M. Dembo, Y. L. Wang, *Biophys. J.* **1999**, *76*, 2307.
- [23] N. Q. Balaban, U. S. Schwarz, D. Riveline, P. Goichberg, G. Tzur, I. Sabanay, D. Mahalu, S. Safran, A. Bershadsky, L. Addadi, B. Geiger, *Nat. Cell Biol.* **2001**, *3*, 466.
- [24] O. du Roure, A. Saez, A. Buguin, R. H. Austin, P. Chavrier, P. Silberzan, B. Ladoux, *Proc. Natl. Acad. Sci. USA* **2005**, *102*, 2390.
- [25] J. Fu, Y. K. Wang, M. T. Yang, R. A. Desai, X. Yu, Z. Liu, C. S. Chen, *Nat. Methods* **2010**, *7*, 733.
- [26] K. T. Bashour, A. Gondarenko, H. Chen, K. Shen, X. Liu, M. Huse, J. C. Hone, L. C. Kam, *Proc. Natl. Acad. Sci. USA* **2014**, *111*, 2241.
- [27] S. Ghassemi, G. Meacci, S. Liu, A. A. Gondarenko, A. Mathur, P. Roca-Cusachs, M. P. Sheetz, J. Hone, *Proc. Natl. Acad. Sci. USA* **2012**, *109*, 5328.
- [28] Y. Li, F. Qian, J. Xiang, C. M. Lieber, *Mater. Today* **2006**, *9*, 18.
- [29] C. Thelander, P. Agarwal, S. Brongersma, J. Eymery, L. F. Feiner, A. Forchel, M. Scheffler, W. Riess, B. J. Ohlsson, U. Gösele, L. Samuelson, *Mater. Today* **2006**, *9*, 28.
- [30] R. Yan, D. Gargas, P. Yang, *Nat. Photonics* **2009**, *3*, 569.
- [31] S. Xu, Y. Qin, C. Xu, Y. Wei, R. Yang, Z. L. Wang, *Nat. Nanotechnol.* **2010**, *5*, 366.
- [32] F. Patolsky, C. M. Lieber, *Mater. Today* **2005**, *8*, 20.
- [33] C. Chiappini, *ACS Sens.* **2017**, *2*, 1086.
- [34] W. Hallstrom, M. Lexholm, D. B. Suyatin, G. Hammarin, D. Hessman, L. Samuelson, L. Montelius, M. Kanje, C. N. Prinz, *Nano Lett.* **2010**, *10*, 782.
- [35] D. Tsviton, M. Schwartzman, R. Popovitz-Biro, E. Joselevich, *ACS Nano* **2012**, *6*, 6433.
- [36] P. Yang, H. Yan, S. Mao, R. Russo, J. Johnson, R. Saykally, N. Morris, J. Pham, R. He, H. J. Choi, *Adv. Funct. Mater.* **2002**, *12*, 323.
- [37] P. W. Sadik, S. J. Pearton, D. P. Norton, E. Lambers, F. Ren, *J. Appl. Phys.* **2007**, *101*, 104514.
- [38] C. L. Perkins, *J. Phys. Chem. C* **2009**, *113*, 18276.
- [39] S. Z. Deng, H. M. Fan, M. Wang, M. R. Zheng, J. B. Yi, R. Q. Wu, H. R. Tan, C. H. Sow, J. Ding, Y. P. Feng, K. P. Loh, *ACS Nano* **2010**, *4*, 495.
- [40] B. Nikoobakht, C. A. Michaels, S. J. Stranick, M. D. Vaudin, *Appl. Phys. Lett.* **2004**, *85*, 3244.
- [41] H. D. Brightbill, D. H. Libraty, S. R. Krutzik, R. B. Yang, J. T. Belisle, J. R. Bleharski, M. Maitland, M. V. Norgard, S. E. Plevy, S. T. Smale, P. J. Brennan, B. R. Bloom, P. J. Godowski, R. L. Modlin, *Science* **1999**, *285*, 732.
- [42] J. Wu, Y. Song, A. B. H. Bakker, S. Bauer, T. Spies, L. L. Lanier, J. H. Phillips, *Science* **1999**, *285*, 730.
- [43] J. L. Upshaw, L. N. Arneson, R. A. Schoon, C. J. Dick, D. D. Billadeau, P. J. Leibson, *Nat. Immunol.* **2006**, *7*, 524.
- [44] S. Gilfillan, E. L. Ho, M. Cella, W. M. Yokohama, M. Colonna, *Nat. Immunol.* **2002**, *3*, 1150.
- [45] W. T. Arthur, L. A. Quilliam, J. A. Cooper, *J. Cell Biol.* **2004**, *167*, 111.
- [46] W.-J. Pannekoek, M. R. H. Kooistra, F. J. T. Zwartkruis, J. L. Bos, *Biochim. Biophys. Acta, Biomembr.* **2009**, *1788*, 790.
- [47] J. Deeg, M. Axmann, J. Matic, A. Liapis, D. Depoil, J. Afrose, S. Curado, M. L. Dustin, J. P. Spatz, *Nano Lett.* **2013**, *13*, 5619.
- [48] D. Delcassian, D. Depoil, D. Rudnicka, M. Liu, D. M. Davis, M. L. Dustin, I. E. Dunlop, *Nano Lett.* **2013**, *13*, 5608.
- [49] Y. Keydar, G. Le Saux, A. Pandey, E. Avishay, N. Bar-Hanin, T. Esti, V. Bhingardive, U. Hadad, A. Porgador, M. Schwartzman, *Nanoscale* **2018**, *10*, 14651.
- [50] R. J. Pelham, Y.-I. Wang, *Proc. Natl. Acad. Sci. USA* **1997**, *94*, 13661.
- [51] P. C. Georges, P. A. Janmey, *J. Appl. Physiol.* **2005**, *98*, 1547.
- [52] H. B. Wang, M. Dembo, Y. L. Wang, S. Ghassemi, G. Meacci, S. Liu, A. Gondarenko, A. Mathur, P. Roca-Cusachs, M. P. Sheetz, J. Hone, J. L. Leight, M. a. Wozniak, S. Chen, M. L. Lynch, S. Christopher, *Am. J. Physiol.: Cell Physiol.* **2000**, *279*, C1345.
- [53] J. Solon, I. Levental, K. Sengupta, P. C. Georges, P. A. Janmey, *Biophys. J.* **2007**, *93*, 4453.
- [54] A. K. Shalek, J. T. Gaubomme, L. Wang, N. Yosef, N. Chevrier, M. S. Andersen, J. T. Robinson, N. Pochet, D. Neuberger, R. S. Gertner, I. Amit, J. R. Brown, N. Hacohen, A. Regev, C. J. Wu, H. Park, *Nano Lett.* **2012**, *12*, 6498.
- [55] Y. R. Na, S. Y. Kim, J. T. Gaubomme, A. K. Shalek, M. Jorgolli, H. Park, E. G. Yang, *Nano Lett.* **2013**, *13*, 153.
- [56] N. Yosef, A. K. Shalek, J. T. Gaubomme, H. Jin, Y. Lee, A. Awasthi, C. Wu, K. Karwacz, S. Xiao, M. Jorgolli, D. Gennert, R. Satija, A. Shakya, D. Y. Lu, J. J. Trombetta, M. R. Pillai, P. J. Ratcliffe, M. L. Coleman, M. Bix, D. Tantin, H. Park, V. K. Kuchroo, A. Regev, *Nature* **2013**, *496*, 461.
- [57] C. N. Prinz, *J. Phys.: Condens. Matter* **2015**, *27*, 233103.
- [58] L. Hanson, Z. C. Lin, C. Xie, Y. Cui, B. Cui, *Nano Lett.* **2012**, *12*, 5815.
- [59] T. Berthing, S. Bonde, K. R. Rostgaard, M. H. Madsen, C. B. Sorensen, J. Nygård, K. L. Martinez, *Nanotechnology* **2012**, *23*, 415102.
- [60] A. M. Xu, A. Aalipour, S. Leal-Ortiz, A. H. Mekhdjian, X. Xie, A. R. Dunn, C. C. Garner, N. A. Melosh, *Nat. Commun.* **2014**, *5*, 3613.
- [61] Ü. Özgür, Y. I. Alivov, C. Liu, A. Teke, M. A. Reshchikov, S. Doan, V. Avrutin, S. J. Cho, H. Morkoç, *J. Appl. Phys.* **2005**, *98*, 041301.
- [62] L. D. Landau, E. M. Lifshitz, *Theory of Elasticity*, Butterworth-Heinemann, Oxford, UK **1986**.
- [63] G. Y. Jing, H. L. Duan, X. M. Sun, Z. S. Zhang, J. Xu, Y. D. Li, J. X. Wang, D. P. Yu, *Phys. Rev. B* **2006**, *73*, 235409.
- [64] Y. Huang, X. Bai, Y. Zhang, *J. Phys. Condens. Matter* **2006**, *18*, L179.
- [65] X. D. Bai, P. X. Gao, Z. L. Wang, E. G. Wang, *Appl. Phys. Lett.* **2003**, *82*, 4806.
- [66] H. Ni, X. Li, *Nanotechnology* **2006**, *17*, 3591.
- [67] J. Song, X. Wang, E. Riedo, Z. L. Wang, *Nano Lett.* **2005**, *5*, 1954.
- [68] H. G. Ljunggren, K. Karre, *Immunol. Today* **1990**, *11*, 237.
- [69] B. Perussia, M. J. Loza, *Trends Immunol.* **2003**, *24*, 235.
- [70] E. O. Long, H. Sik Kim, D. Liu, M. E. Peterson, S. Rajagopalan, *Annu. Rev. Immunol.* **2013**, *31*, 227.
- [71] O. Matalon, A. Ben-Shmuel, J. Kivelevitz, B. Sabag, S. Fried, N. Joseph, E. Noy, G. Biber, M. Barda-Saad, *EMBO J.* **2018**, *37*, e96264.
- [72] E. Aktas, U. C. Kucuksezer, S. Bilgic, G. Erten, G. Deniz, *Cell. Immunol.* **2009**, *254*, 149.
- [73] G. Alter, J. M. Malenfant, M. Altfeld, *J. Immunol. Methods* **2004**, *294*, 15.
- [74] M. Bruchard, G. Mignot, V. Derangère, F. Chalmin, A. Chevriaux, F. Végran, W. Boireau, B. Simon, B. Ryffel, J. L. Connat, J. Kanellopoulos, F. Martin, C. Rébé, L. Apetoh, F. Ghiringhelli, *Nat. Med.* **2013**, *19*, 57.
- [75] K. Krzewski, A. Gil-Krzewska, V. Nguyen, G. Peruzzi, J. E. Coligan, *Blood* **2013**, *121*, 4672.
- [76] F. Bertrand, S. Muller, K.-H. Roh, C. Laurent, L. Dupre, S. Valitutti, *Proc. Natl. Acad. Sci. USA* **2013**, *110*, 6073.

- [77] R. S. O'Connor, X. Hao, K. Shen, K. Bashour, T. Akimova, W. W. Hancock, L. C. Kam, M. C. Milone, *J. Immunol.* **2012**, *189*, 1330.
- [78] Z. Wan, S. Zhang, Y. Fan, K. Liu, F. Du, A. M. Davey, H. Zhang, W. Han, C. Xiong, W. Liu, *J. Immunol.* **2013**, *190*, 4661.
- [79] K. T. Roybal, L. J. Rupp, L. Morsut, W. J. Walker, K. A. McNally, J. S. Park, W. A. Lim, *Cell* **2016**, *164*, 770.
- [80] C. C. Kloss, M. Condomines, M. Cartellieri, M. Bachmann, M. Sadelain, *Nat. Biotechnol.* **2013**, *31*, 71.
- [81] M. Themeli, M. Sadelain, *Trends Mol. Med.* **2016**, *22*, 271.
- [82] Z. Li, H. Persson, K. Adolfsson, S. Oredsson, C. N. Prinz, *Sci. China: Life Sci.* **2018**, *61*, 427.
- [83] A. K. Shalek, J. T. Robinson, E. S. Karp, J. S. Lee, D.-R. Ahn, M.-H. Yoon, A. Sutton, M. Jorgolli, R. S. Gertner, T. S. Gujral, G. MacBeath, E. G. Yang, H. Park, *Proc. Natl. Acad. Sci. USA* **2010**, *107*, 1870.
- [84] J. Dolbow, M. Gosz, *Mech. Mater.* **1996**, *23*, 311.
- [85] E. M. Mace, J. S. Orange, *Front. Immunol.* **2012**, *3*, 421.
- [86] M. J. P. Biggs, M. C. Milone, L. C. Santos, A. Gondarenko, S. J. Wind, *J. R. Soc., Interface* **2011**, *8*, 1462.
- [87] C. Borg, J. Abdelali, D. Laderach, K. Maruyama, H. Wakasugi, S. Charrier, B. Ryffel, W. Vainchenker, A. Galy, A. Caignard, L. Zitvogel, A. Cambi, C. Figdor, *Blood* **2004**, *104*, 3267.
- [88] P. Verdijk, P. A. van Veelen, A. H. de Ru, P. J. Hensbergen, K. Mizuno, H. K. Koerten, F. Koning, C. P. Tensen, A. M. Mommaas, *Eur. J. Immunol.* **2004**, *34*, 156.
- [89] M. Granzin, J. Wagner, U. Köhl, A. Cerwenka, V. Huppert, E. Ullrich, *Front. Immunol.* **2017**, *8*, 458.